VOL. 18, NO. 9, MAY 2023 ISSN 1819-6608
ARPN Journal of Engineering and Applied Sciences

www.arpnjournals.com

EVALUATION OF THE LEVEL OF DAMAGE TO THERMOPLASTIC FLAT SHEETS OF ACRYLONITRILE BUTADIENE STYRENE (ABS) SUBJECTED TO STATIC TENSILE TESTS USING STATIC AND UNIFIED DAMAGE AND ESTIMATION OF SERVICE LIFE

Abderrazak En-Naji[1,2], M. Lahlou[3], Gh. Arid[2], A. Khtibari[4], L. Souinida[1], N. Mouhib[2] and A. Daya[1]
[1]Department of Physics, Laboratory M3ER, Faculty of Sciences and Technology, Moulay Ismail University, Meknes, Morocco
[2]National Higher School of Electricity and Mechanics, Laboratory of Control and Mechanical Characterization of Materials and Structures, BP Oasis, Hassan II University, Casablanca, Morocco
[3]labSIPE, (ENSAJ) University Chouaibdoukkali, El Jadida, Morocco
[4]Condensed Matter Physics Laboratory, Faculty of Sciences Ben M'Sick, University Hassan II of Casablanca, Casablanca, Morocco
E-Mail: abdenaji14@gmail.com

ABSTRACT

In this study, we are interested in the characterization of a flat plate in polymeric ABS under the uniaxial solicitation. We ran a series of tests on smooth rectangular specimens (defect-free) by ASTM 882-02 standards to characterize the material and provide a scale of comparison, as well as to investigate the combined defect effect on the mechanical behavior of ABS. Another panoply of tests was performed on rectangular test pieces with holes with a single notch and holes with a double notch. Then, we experimentally identify the propagation of their damage. The calculation of the damage, using models of experimental damage, led to determining the three stages of the evolution of the damage, which are the initiation, propagation, and complete deterioration of the material. Therefore, the approach of reliability (R) is a statical parameter, used to designate the critical life fraction concerning the notch depth (βc) of a modeled defect as a combined defect on an ABS specimen. In addition, the unified theory was developed in this context, on the one hand, to define the damage parameter, which is the internal variable that describes the state of damage of the structure in terms of the life fraction, and on the other hand for the theoretical re-evaluation of the level of damage. These techniques have the advantage of quickly assessing the performance and stability of the studied polymer and deciding whether to have an anticipatory maintenance strategy and an awareness of the safety requirements policy regarding the damage-reliability behavior of the studied specimens. From the latter, the discussion of the curves allowed us to maintain the limits of the ABS materials' mechanical behavior and confirmed that the theoretical and experimental results show good agreement and correlation.

Keywords: ABS, damage, mechanical behavior, stress, sudden rupture, tensile testing.

Manuscript Received 24 January 2023; Revised 26 June 2023; Published 30 June 2023

1. INTRODUCTION

Prediction and evaluation of mechanical behavior have long been serious concerns. Thus, many models have been developed in the literature to quantify the damage caused by steel materials, either by reference to linear or non-linear models [1]. Miner was the first author to mathematically formulate a fatigue damage law [2]. Its linear formulation of the damage as a function of the fraction of the total work absorbed by the material makes it a simple and obvious law to use. Other authors, including Bui Quoc [3], proposed modeling of the damage depending on the loading conditions, the level of stress, the stress frequency, and the characteristics of the material. The models of Henry [4], Lemaitre, and Chaboche [5], or of Gatt [6], can also be cited as presentations of the damage. There has been much application of prior theories to steel materials and their alloys [7]. We plan to apply these theories to an ABS thermoplastic polymer to benefit from them. Thus, several studies have been launched on this material to quantify its mechanical behavior. Gonzalo *et al.* [8] evaluated the influence of the fatigue ultrasonic of ABS (acrylonitrile-butadiene-styrene) and the crack propagation mechanism when the test specimens are submerged in oil and water, to limit the temperature increase resulting from the intense mechanical vibration employed in ultrasonic fatigue testing. The toxicology of ABS combustion products was examined by Joseph V. and al. [9]. When T. J. Bohatka and al. [10] examined the variability in damage production during fatigue crack propagation in ABS materials, they found that these variations were related to variations in fracture propagation behavior via the crack layer. The ABS material was subjected to several combined cycles of extrusion and aging in the air at a high temperature when Boldizar *et al.* [11] examined the degradation of ABS during multiple treatments and accelerated aging. Changes in the mechanical flow and tensile characteristics were found. While the extrusion step takes place between the third and seventh cycles, the elongation modulus at break falls with aging.

In the framework of damage mechanics, several researchers developed theoretical expressions of static

damage like Starkey, Miner, and Shanly. Biu-Quoc has developed the model of the unified theory of metal fatigue and suggested expressions of static damage that permit quantification of the progression of the static damage according to the initial and present fatigue limits. To use this model for polymers' characterization, through static tests, it needs judicious adaptation, taking into account different parameters. However, GHANIM *et al*. [12] used the standardized damage to characterize an acrylonitrile-butadiene-styrene (ABS) polymer plate under uniaxial loading. Arid and al [13] used a standardized degradation formulation on notched test pieces made of rigid PVC. To draw attention to how the notch affects the behavior of pipes, Majid *et al*. [14] adapted the theories of rupture pressure to the case of high-density polyethylene (HDPE). And finally, many studies have been done by EN-NAJI et al. (2019) [15], who have conducted several investigations. They investigated the use of a newly developed non-linear damage reliability to examine the impact of rising temperature on the behavior of ABS, as well as the mechanical characterization and failure analysis of ABS during static testing with temperature effects [16], and, the experimental prediction of the service life of ABS by the Energy Method [17].

This research focuses on the characterization of a polymeric ABS flat plate that has been sliced under uniaxial stress. The damage to ABS flat plates cut under uniaxial stress is defined and assessed using a unified damage theory. Our primary objective is to examine stress concentration characteristics and how they impact the degree of damage to notched structures.

2. MATERIAL AND EXPERIMENTAL METHODS

ABS (Acrylonitrile Butadiene Styrene) is a polymer amorphous created when acrylonitrile and styrene are emulsified or mass-polymerized in the presence of a polybutadiene emulsion. It is defined by three properties main: impact resistance, hardness, and heat resistance. To characterize this material a series of tests were carried out on dumbbell test specimens according to ASTM D638-03 [18], the specimen's geometry and dimensions are shown in Figure-1.

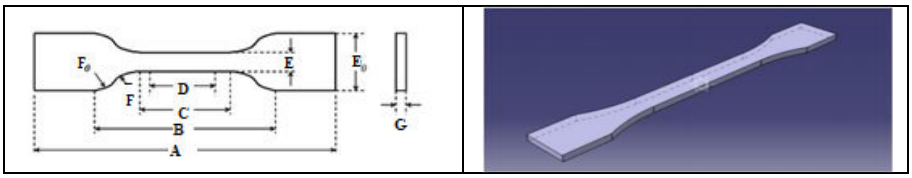

Figure-1. Shows ABS specimen dimensions and geometry by ASTM D638-03.

Table-1. Lists the specs for the dumbbell specimen used in the tensile test.

Symbol	Description	Dimensions accuracy of ±0.1mm
A	Total length	75.1
B	The initial distance between jaws	42.1
C	Length of the calibrated part	25.1
D	Length between landmarks	20.1
E	With the specimen	4.1
F	Small radius of curvature	8.1
E_0	Widths at the ends	14.1
G	The thickness of the specimen	2.1

Figure-2 shows the evolution of the stress (MPa) applied to the specimens as a function of the deformation (%). Based on how it appears as a whole, this curve has displayed ductile behavior.

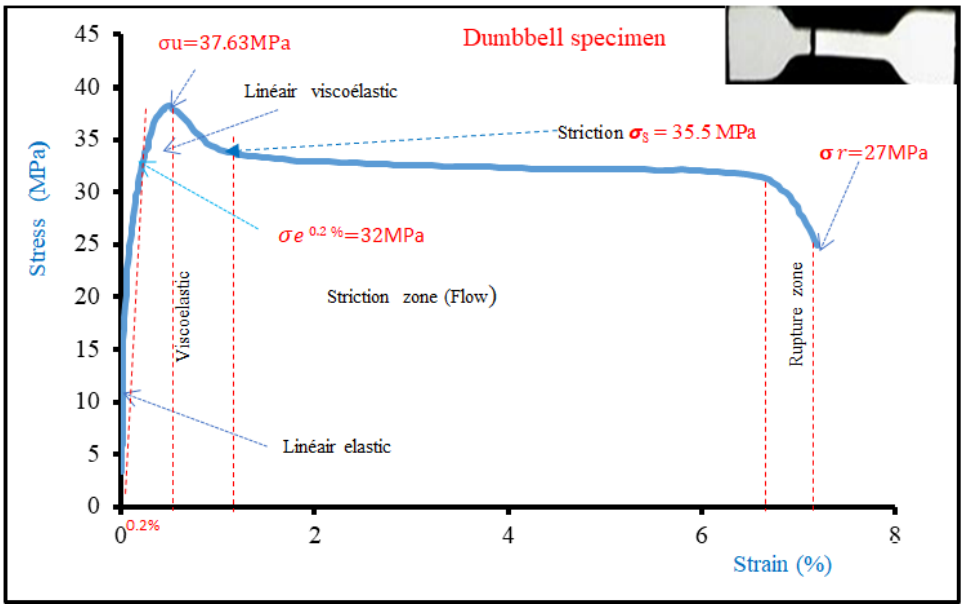

Figure-2. Tensile curve stress-deformation dumbbell specimen.

We notice from Figure-2 that the curve has five zones. Each of these areas reveals a particular mechanical behavior of the polymer (ABS) during the tensile test.

Zone 1 (linear): this is the reversible elastic deformation of the ABS material due to the amorphous phase.

Zone 2: As the force decreases, it is the beginning of the deformation, which corresponds to a heterogeneous deformation of the material.

Zone 3: extending the specimen's zone of constriction until stability.

Zone 4: As the stretching force rises, the deformation returns to being homogeneous due to a structural hardening associated with the alignment of the macromolecular chains in the direction of stretching and the rise in the fibrillar fraction of the ABS material until breakage.

We were able to ascertain the mechanical characteristics of the material under study thanks to the outcomes depicted in Figure-2. The elastic modulus, elastic limit, and breaking stress are some examples of these properties, and they are all mentioned in Table-2.

Table-2. Outlines the mechanical properties of ABS.

Elastic modulus	Poisson's ratio	Elastic limit	Ultimate stress
E = 2.08 GPa	υ = 0.33	σe = 32MPa	σu = 37.63 MPa

2.1 Operational Method

The experimental part entails submitting smooth, rectangular specimens (defect-free) to characterize the material and provide a scale of comparison, as well as to investigate the effect of the combined defect. Another series of tests have been performed on rectangular specimens pierced with a single notch and another pierced with a double notch, with diameters ranging from 2 mm up to 30 mm and a pitch of 3 mm, and with a fixed notch of 1 mm. To highlight the influence of combined defects on the behavior of the test pieces, it should be noted that the tests were conducted according to ASTM 882-02 [19] and ASTM D 5766 M [20]. Test pieces with varying diameters that have been simply twisted and double-notched are shown in Figures 3 and 4; a test piece that has been secured against the traction machine's jaws is shown in Figure-5.

Figure-3. Rectangular specimens with a combined defect: hole plus single notch and hole plus double notch.

Figure-4. Specimens with a combined defect after testing.

2.2 Experimental Apparatus

Tensile tests were performed to characterize the monotonic properties of the ABS material using a Zwick-Roell machine with a maximum load capacity of 2.5 KN, which allowed us to obtain a higher degree of precision in our testing, given the nature of the test material and the dimensions and geometry of the test pieces, which have a small thickness. The tests were performed at a uniform speed of 1 mm per minute with controlled movement. Figure-5 depicts the specimen positioned up against the traction machine's jaws.

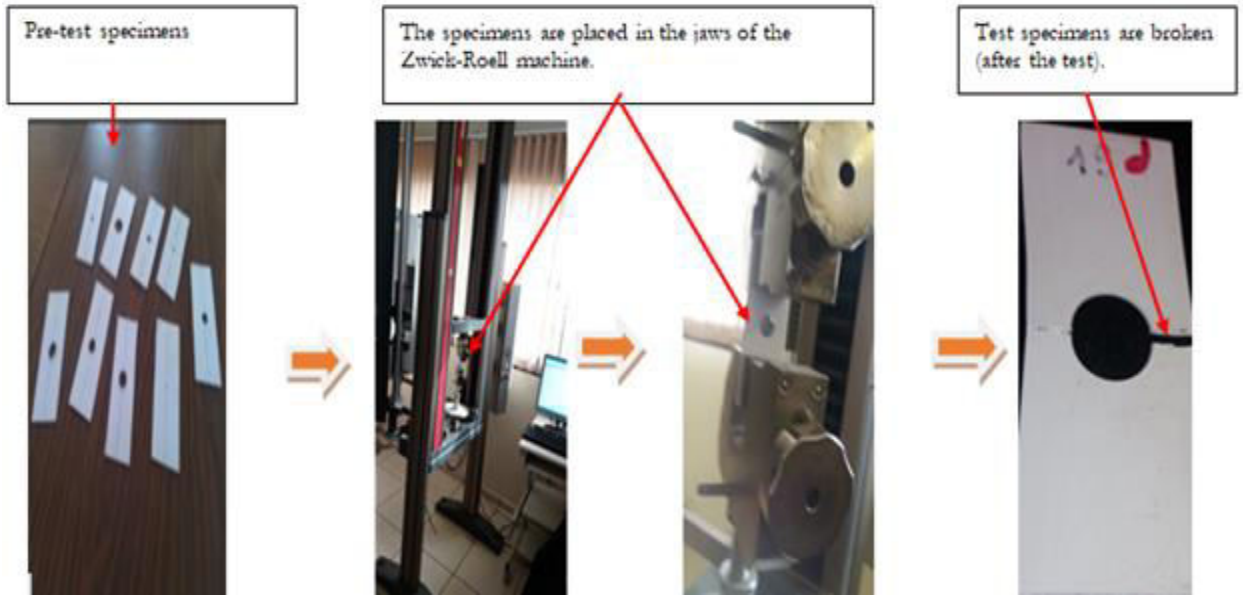

Figure-5. Shows the experimental setup and test specimens.

3. THEORY

3.1 Rupture Resistance Theories

To forecast a component's life and prevent any catastrophic breakdown in service, it is crucial to be aware of its properties and mechanical behavior. This backdrop informs our study, which examines the dependability of intentionally damaged structures. The study is based on the evaluation of the amount of damage, and a calculation of the damage will be undertaken in this paragraph to better understand the mechanism of damage to these structures. To model damage in structural computation, various models are offered. The Minner model is the damage model that is most frequently utilized [21, 22]. There are limitations as a result of its linear depiction of cumulative damage progression, which does not adequately indicate the status of the structure's degradation. The models of Miller [23] and Chaboche [24] are two more suggested techniques that have attempted to modify this model to depict damage more appropriately. Indeed, several writers, including Bui Quoc [25], have suggested modeling the damage based on the loading circumstances, the amount of stress, the frequency of stress, and the properties of the virgin material. The models of Henry [26], Lemaitre and Chaboche [27], and Gatt [28] can be used as examples of damage.

3.2 Unified Theory

When a material is subjected to fatigue, its physical properties frequently deteriorate. The exact cornerstones of the unified theory are the narrowing of the fatigue limit and the decrease in material resistance [29-37]. According to this theory, when the mean stress is zero, the rate of variation of the limit of endurance is expressed as a function of the number of periods used as follows:

$$\frac{d\sigma_e}{dn} = \frac{1}{k_f}\gamma^a(\gamma-\gamma_e)^2$$

$$\gamma = \frac{\Delta\sigma}{\sigma_a} \quad ; \quad \gamma_e = \frac{\sigma_e}{\sigma_a}$$

With Δσ loading amplitude, σ_0 endurance limit of virgin material, n Number of applied fatigue cycles, kf, and, a constant of the ABS material.

This expression's integration requires consideration of the boundary conditions established by:

$\gamma e = 1$ si $n = 0$
$\gamma e = (\Delta\sigma / \sigma u)^m = 0$ si $n = N_f$

In this case, the critical diameter of the hole is represented by Nf, the number of cycles to failure for a fatigue test, and m, an empirical material constant.

$$N_f = \frac{k}{\gamma^a}\left[\frac{1}{\gamma - 1} - \frac{1}{\gamma - \left(\frac{\gamma}{\gamma_u}\right)^m}\right]$$

The instantaneous value of the endurance limit determines the damage given by:

$$D = \frac{1 - \gamma_e}{1 - \gamma_e^*}$$

By setting posing β=n/Nf this theory leads to the following equation:

$$D_{th} = \frac{\beta}{\beta + (1-\beta)\left[\frac{\gamma - (\gamma/\gamma_u)^m}{\gamma - 1}\right]} \quad (1)$$

A correlation between monotonic tensile strength and cyclic loading is provided by the Bui Quoc model. If a material has undergone cyclical efforts before the application of a static force, its resistance to that force will be reduced. Here, we're referring to the material's declining residual resistance. The aforementioned model's proposed rate of loss of the residual ultimate stress is shown by:

$$\frac{\sigma_{ur}}{\sigma_u} = \left[\gamma - \frac{1}{\frac{1-\beta}{\gamma - 1} + \frac{\beta}{\gamma - \left(\frac{\gamma}{\gamma_u}\right)^m}}\right]^{1/m} \quad (2)$$

Where the various terms are successive:
$\gamma_e = \frac{\sigma_e}{\sigma_a}$:Non-dimension alendurence limit
$\gamma u = \frac{\sigma u}{\sigma a}$:Non-dimensional cyclic stress
$\gamma = \frac{\sigma ur}{\sigma a}$: Instantaneous non-dimensional endurance limit
σu : Maximum endurance of virgin material
σur : is the residual ultimate stress of the material at different hole diameters
σa : Applied stress level
and : m; is a material parameter, with m = 1 for amorphous polymers according to [14-17,31-39].

3.3 Damage Experimental

Experimental damage involves determining the progression of the ultimate residual stress, the fluctuations of which are fundamentally due to the damage. Indeed, we used the static damage variable for each life fraction, so by analogy with the theory shown above, the life fraction of our study represents the relation between the progression of the diameter of the hole and its critical value. The advantage of this theory is that it directly relates the damage to the ABS material's characteristics, as well as the progression of the damage to the variation of the ultimate residual limit. The variable "static damage" can be defined as follows:

$$D = \frac{1 - \frac{\sigma_{ur}}{\sigma_U}}{1 - \frac{\sigma_a}{\sigma_U}} \quad (3)$$

D = 0: if the specimen has not been subjected to any preliminary damage (when σur = σu).
D = 1: if the specimen is failed (when σur= σa).

4. DAMAGE- RELIABILITY

When an ABS material is subjected to static stress, its physical properties deteriorate gradually. There is often a need to reduce the probability of sudden failure. And consequently, reliability assessment becomes indispensable in any study of the mechanical behavior of the components. In this section, we will present a reliable study to reduce the probability of sudden failure. The static reliability R is a statistical parameter that follows the evolution of the deterioration of the material. The relationship between these two parameters can be written as follows: R (β) + D (β) = 1 (4) [14-17, 31-39]. Using equation 4 to plot the different reliability curves that correspond to the different parameters studied, the following figures illustrate the variation in reliability and damage as a function of the life fraction β. We note that the damage always evolves in the opposite direction with reliability because the depth of the notch increases.

5. RESULTS AND DISCUSSIONS

The curves obtained from the tests performed on perforated rectangular specimens that were simply notched, perforated, and doubly notched are shown, respectively, in Figures 6 and 7. We noticed that the crack propagates progressively until the complete rupture of the test specimens. Each of these curves begins with an elastic linear part, followed by a continuous distance from the real curve to the ideal load/displacement line. This nonlinearity is mainly due to the plasticization of the area located near the tip of the crack and the fact that the crack tends to propagate suddenly with a jolt of very low intensity. Then the sudden drop in the load/displacement curve corresponds to the breaking load of the specimen.

It is noted on these curves that the degradation of the mechanical properties of the elastic stress, the ultimate stress, the stress at break, and the elongation is consistently striking. If we consider the results to be decreasingly decreasing with increasing hole diameter, we no longer see a stress stability zone or significant elongation. Local plasticization frequently comes first, followed by the rupture, and then an abrupt break.

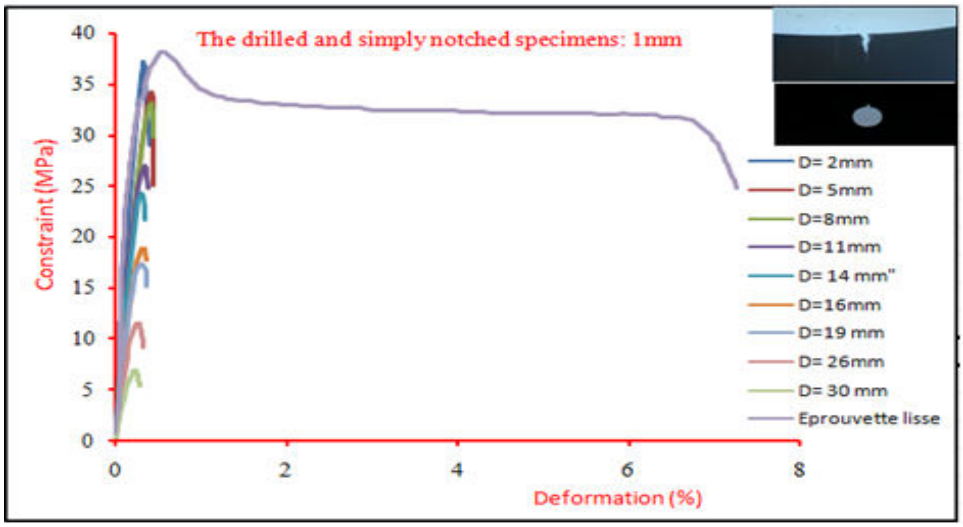

Figure-6. Depicts the evolution of the stress-strain curves for uniaxial tensile tests on rectangular test specimens with hole diameters ranging from 2 mm to 30 mm and a simple notch, as specified by ASTM D 882-02 and ASTM D5766M.

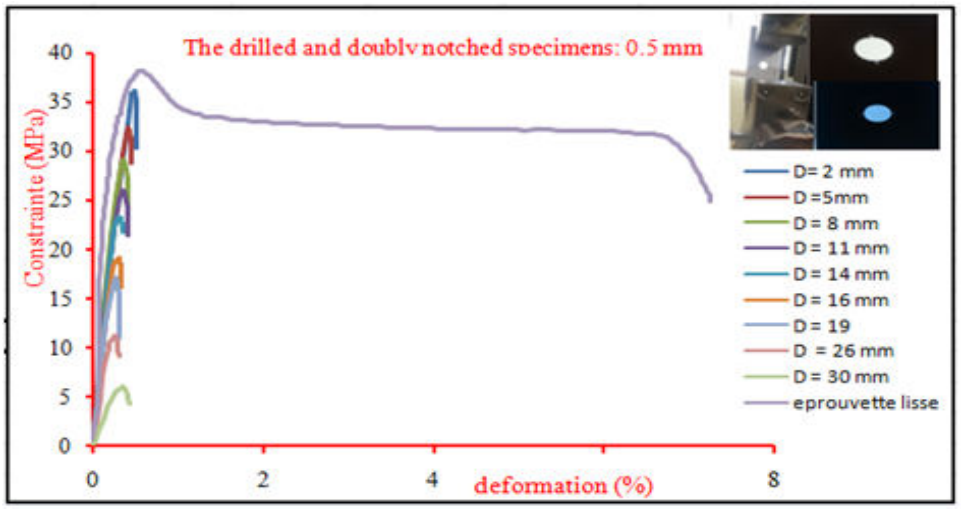

Figure-7. Depicts the evolution of the stress-strain curves for uniaxial tensile tests on rectangular test specimens with hole diameters ranging from 2 mm to 30 mm and a double notch, as specified by ASTM D 882-02 and ASTM D5766M.

In carrying out the tests and according to the results shown in Figures 6 and 7, it has been found that the maximum loading is obtained with the same displacement of the lips of the crack. This load is even higher than the hole diameter is small. The damaged specimens exhibit an elastic linear behavior with the appearance of a small non-linearity. This non-linearity can be related to the decrease of the real section during the test (striction) by the progressive rupture of the fibers. Following the rupture of a large number of fibers, the stress decreases abruptly, and the size of the damaged area is all the more important than the diameter of the hole being weak. Figure-8 depicts the decrease in the maximum loads during crack propagation.

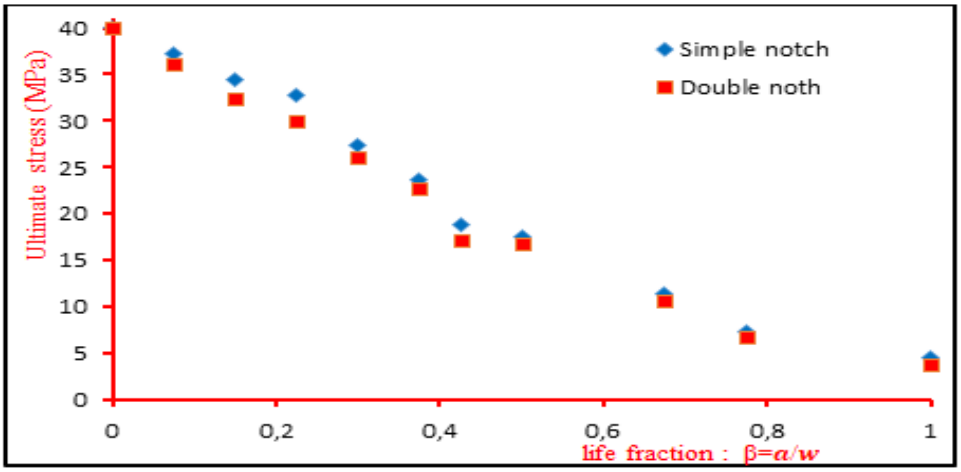

Figure-8. Shows an identification of the development of the maximum stress between perforated specimens with a single notch and those with two-notch configurations based on the diameter of the hole.

Dumbbell specimens at room temperature can withstand an ultimate stress σu = 37.68 MPa. As the reduction in thickness increases, the final residual stresses decrease gradually. This is explained by a loss of strength in ABS materials due to increased defects.

These curves show a remarkable deterioration of the mechanical properties of the material with an increase in hole diameter; these properties include elastic stress, ultimate stress, failure stress, and elongation; the characteristics decrease as long as the hole diameter increases. Consequently, the comparison of the evolution of the maximum resistance between the perforated specimens, simply notched, and the perforated specimens that were doubly notched shows that the test specimens that were simply notched resist better than the doubly notched specimens, especially for diameters less than 22mm. Figure-8 shows the comparison of the evolution of the ultimate nondimensional stress between the perforated specimens, simply notched, and the perforated specimens, doubly notched, according to the diameter of the hole.

5.1 Adimensional Mechanical Property Loss in Relation to the Life Fraction

In this part, we will highlight the experimental resistance loss of the residual ultimate tensile stress (σur) of artificially damaged specimens with a combined defect: a hole with a single notch and a hole with a double notch, depending on the fraction β = a/w. We will particularly focus on comparing the loss rate curves σur/σu (σur: residual ultimate stress, σu: ultimate stress of virgin material) according to the expression of β used.

The curves in Figure-9 show the evolution of the loss of resistance as a function of the life fraction β = a/w (a = length of the notch and w = width of the specimen), degrading in a random way as the life fraction grows until it spreads. The state of the ABS material corresponding to β = 1 is specified by the amplitude of the constraint applied to the fracture and the limit, equivalent to a monotonic test.

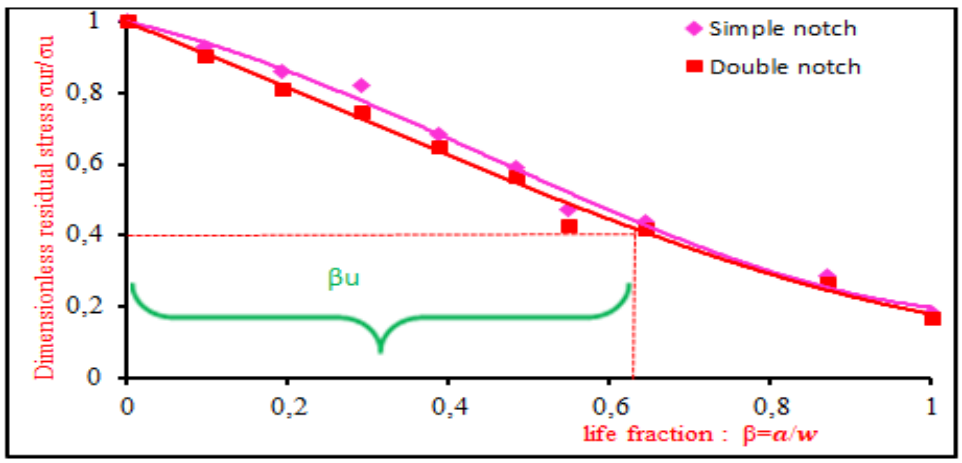

Figure-9. Compares the final nondimensional stress degradation between perforated specimens with a single and double notch, depending on the size of the hole.

The analysis of the curve in Figure-9 shows that the dimensionless strength drops significantly depending on the life fraction, and we find that the loss of strength is very aggressive for a large of the life fraction.

We also note that the dimensionless stress of all specimens is less than 40% (a safety factor of 2.5) when the fraction of life is equal to 60%. Because of this, we define the proportion of usable life (u = a/wu) as the ratio of the useful specimens' notch length to their width (2.5 is the safety factor).

.

5.2 Theoretical and Experimental Detection of Deterioration of Adimensional Mechanical Properties

By analogy with the modified Bui Quoc law [3], the mathematical expression (2) has been exploited to describe the adimensional loss rate of the mechanical properties as a function of the fraction of life and to give a benchmark for comparison between the present theory and the experimental results. Figures 10 and 11 below provide the graphical representations of the theoretical adimensional loss of mechanical properties about the experimental loss.

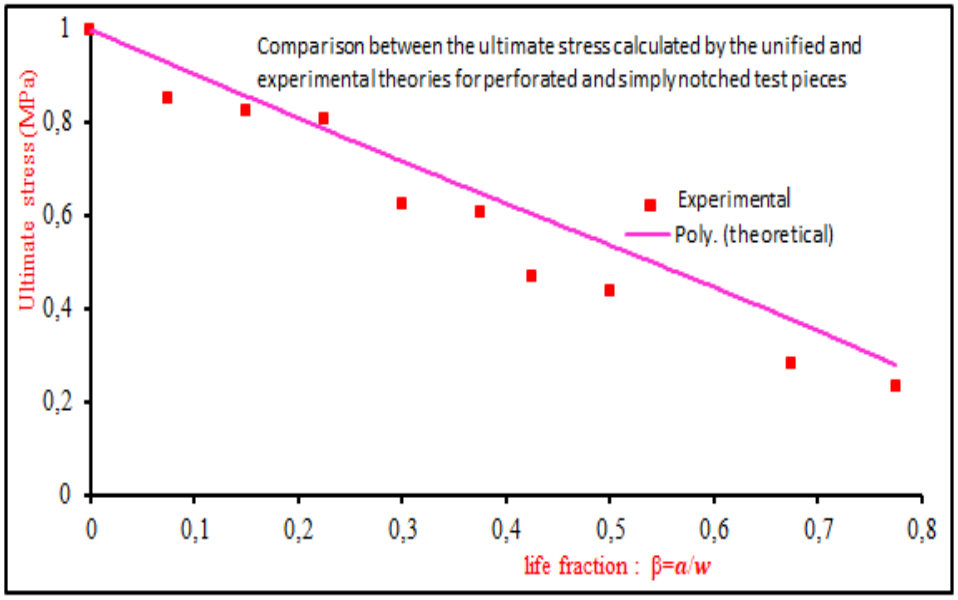

Figure-10. Reveals a correlation between the ultimate stress determined by the unified and experimental theories for perforated and simply notched test pieces.

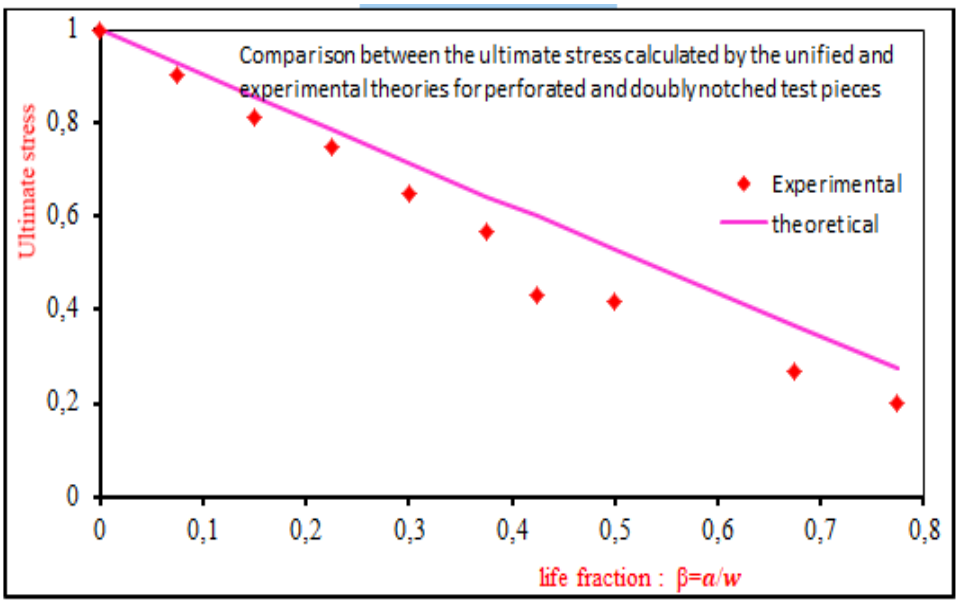

Figure-11. Reveals a correlation between the ultimate stress determined by the unified and experimental theories for perforated and doubly notched test pieces.

5.3 Determination of Static Damage (Experimental)

After determining the stress just before breaking and comparing the theoretical and experimental ultimate stresses for all the test pieces studied, we will use the expression (3) to plot the damage curves. Figures 12, 13, and 14 illustrate the behavior of the static damage between the undamaged test piece in its virgin state, which corresponds to zero damage, and the damaged test specimen, whose damage is equal to 1, and this is for each type of defect.

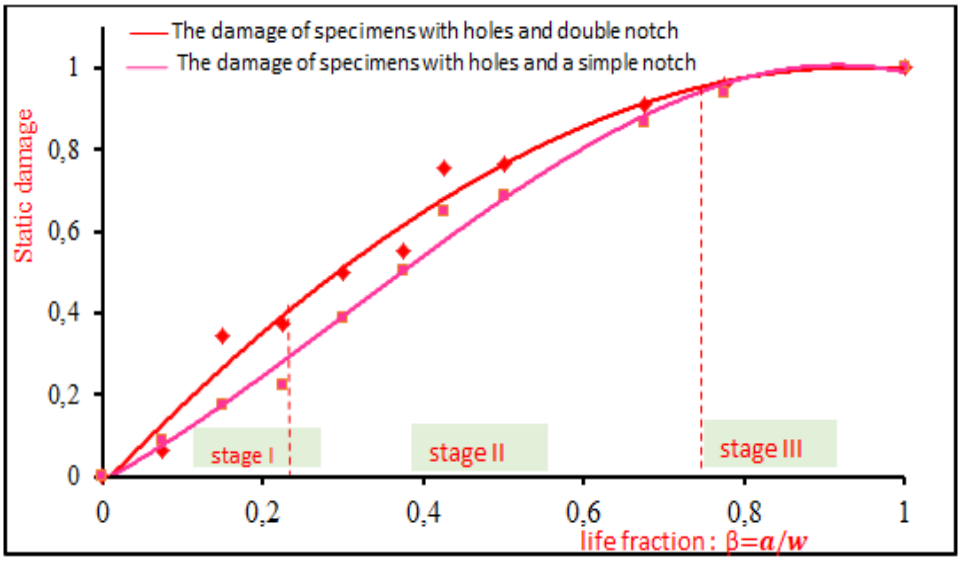

Figure-12. Shows a comparison of the damage propagation in specimens drilled with a single notch and specimens drilled with double notches based on the fraction of life.

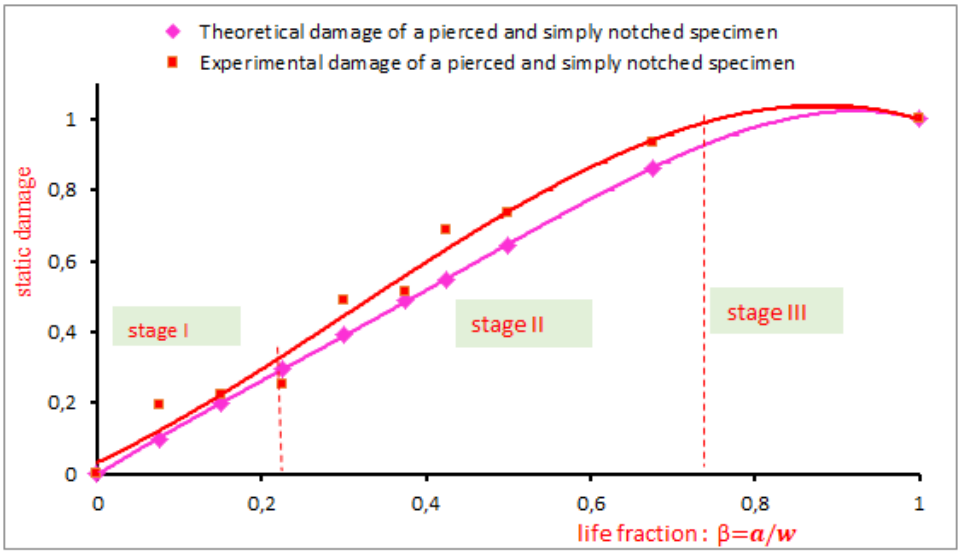

Figure-13. Compares experimental and theoretical damage to test specimens with a simple notch about the life percentage.

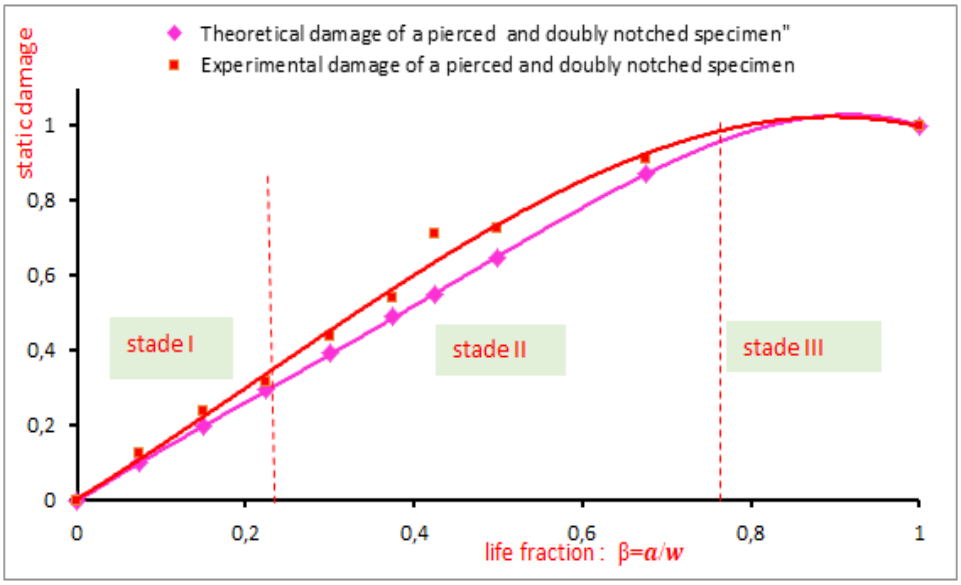

Figure-14. Compares experimental and theoretical damage to test specimens with a double-notch about the life percentage.

Figures 12, 13, and 14 show the damage process as a concave curve, which indicates that the break will occur on D = 1 and that the damage will accelerate as the polymer ABS reaches the end of its useful life. The static tensile strength loss of the ABS test specimens increases as the damage progresses. When the diameter of the hole grows significantly, this loss progresses. This can be explained by the fact that minimal energy can break the specimen when a significant portion of the fibers (about 71%) is broken. This type of damage results in a significant amount of irreversible strain, which lowers the material's maximum strength. In addition, we note that the damage curve of the pierced and doubly notched specimen is above that of the pierced and simply notched specimen, and especially in the first two stages, this reflects the rapid evolution of the level of damage to the pierced test specimen with a double notch compared to that pierced with a simple notch. From critical life fraction βc announces the beginning of stage III, almost all the curves are confused, it is about the unstable phase. The damage becomes uncontrollable, and the test pieces can at any moment manifest a sudden break.

When compared to Stage I, which represents the zone of so-called elastic damage, is the safe zone where the advanced defect of the test piece studied can be controlled. Note that the simple notch is less critical compared to the double notch.

These findings allow us to conclude that the doubly-notched test specimen is the most fragile. This mainly comes down to the distribution of the stresses at the test specimens, where a high concentration of stresses at the notches of the pierced and doubly-cut test piece is noted. whereas, for example, for the pierced and simply notched specimen, this concentration is localized only in one part. Therefore, and in our case, the most tolerable combined defect is the hole with a single notch when it has a longer life.

A static characteristic, on the other hand, enables one to track the progression of the material's deterioration. It is the reliability parameter "R," which stands for the likelihood that the substance would survive [14-17, 31-36].

5.4 Static Reliability and Damage

To assess the relation between static reliability and damage from the values of the ultimate stress, we used model number 4 presented in the theoretical part of this article, this model allowed us to plot the curve of the variation in the superimposed reliability to that of damage for the test-pieces pierced with a simple notch and the test-pieces pierced with a double notch (Figure-15).

By crossing the static damage-reliability curves of ABS specimens, Figure-15, we define precisely the critical life fraction of these pieces pierced with a simple notch, which is represented by βc50% (50%). We can also define the three stages of damage evolution from commencement (stage I [0, 28%]) using this curve, propagation (stage II [28%-74%]), and acceleration (stage III [74%-100%]) of it.

For the test pieces pierced with a double notch, we crossed the static damage-reliability curves, and we find out the critical life fraction of this material, βc2 (50%). From this curve also, the stages of damage correspond to initiation (stage I [0, 23%]), propagation (stage II [23%-67%]), and acceleration (stage III [67%-100%]) of it.

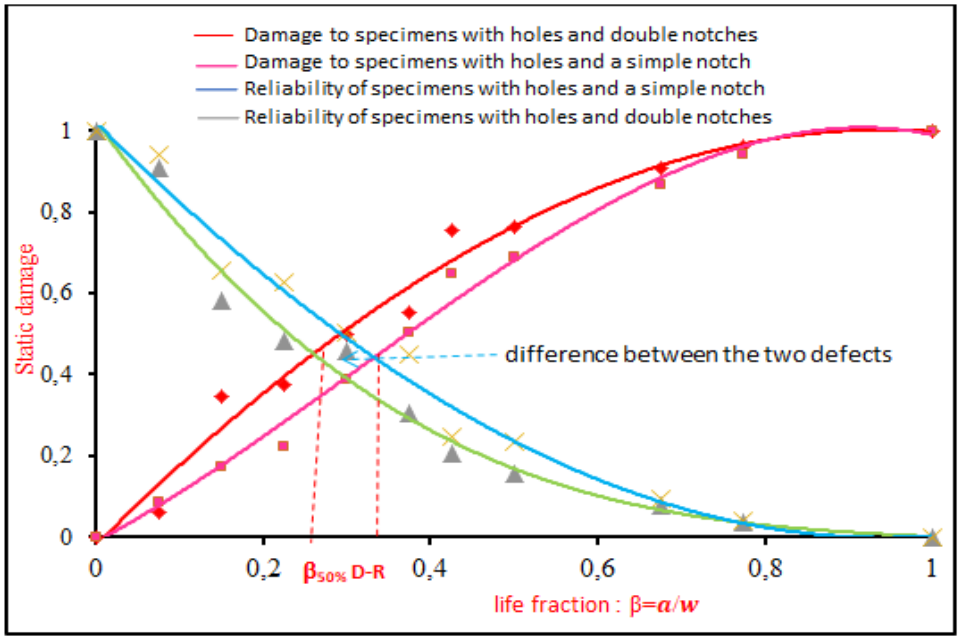

Figure-15. Shows the two test pieces' processed static damage-static reliability (Test Pieces Drilled with a Single Notch and Test Pieces Drilled with a Double Notch).

It is evident from the preceding graph that the reliability curves evolve at a similar rate as the damage curves but in the opposite direction. This leads to the fourth relation, which connects the two numbers.

The superposition of the curve's static damage and static reliability indicates a critical intersection point that coincides with an inversion of the situation. Indeed, the reliability was initially greater than the damage and becomes weaker beyond this point, which corresponds to the acceleration of damage.

This figure depicts that reliability (damage) is high (minimum) at the start of life and rapidly decreases (grows) until the initiation period, which is the junction of the two curves. The priming phase is the longest and most stable phase, and it follows this point where the slope of the two curves reduces and the evolution of the two curves slows down. The structure is destroyed in the last phase, which is also the shortest and most fragile, and the evolution quickens. These curves' arrangement made it possible to identify the various damage stages for the various test items examined.

Stage I: The damage has just started, and it is expanding very slowly at this point. The damage develops linearly and accounts for 22% to 34% of the material-level damage, which means that the specimen starts to lose its internal resistance.

Stage II: It corresponds to the longest and most stable phase of the damage, the phase in which we reach the critical fraction of life 68%. At this stage, the damage for the second stage oscillates between 22% and 74%. Additionally, we see that the two curves cross in the same way throughout every interval of this stage. At this stage, the damage becomes progressive and unsafe, so predictive maintenance is essential for engineering and industry.

Stage III: The third and final phase of the life cycle corresponds to the unstable stage of static damage; the test material is prone to rupture at any time due to sudden, total failure.

The raising of the life fractions, namely, the life fraction of initiation and the fraction of critical life, allowed us to detect whether the damage is stable or not. Knowing this, we can predict the time for maintenance and replacement of the material. These phases are considered the limits that determine the different phases of life of a structure, and this is for the different forms of studied defects:

Types of defect	Stage I	Stage II	Stage III
Hole with a Simple notch	β Є [0%, 28%]	β Є [28%, 74%]	β Є [74%, 100%]
Hole with a double notch	β Є [0%, 23%]	βЄ [23%, 67%]	β Є [67%, 100%]

5.5 Damage Assessment Utilizing the Unified Theory

From all the obtained loads, we were able to establish the damage evolution for each defect, for pierced and simply notched specimens, and for pierced and doubly notched specimens in our case. We modified the unified theory of damage, initially established for metals, to meet

the ABS polymer specifications through the use of the load parameter. The damage is represented by equation (1), a non-linear damage model representing the damage progress for each hole diameter in the function of the life fraction β. Figures (16) and (17), respectively, demonstrate the outcomes.

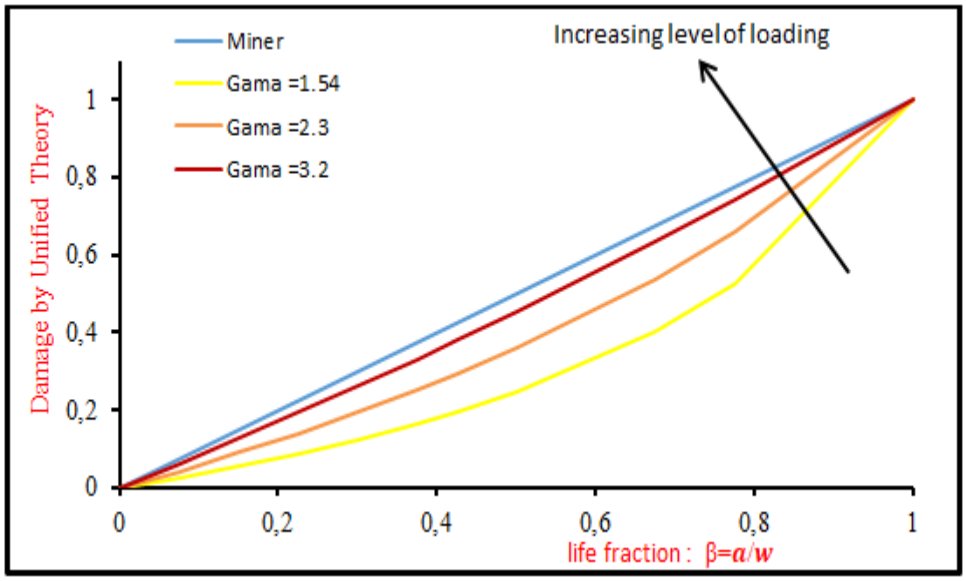

Figure-16. Shows the damage history of test specimens with a simple notch using the unified theory and Miner law and according to the life percentage.

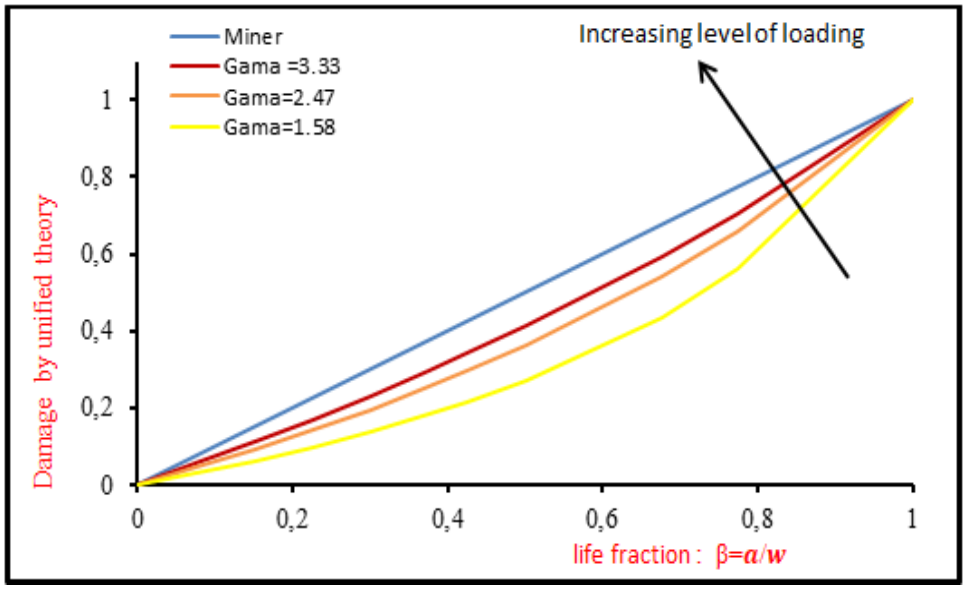

Figure-17. Shows the damage history of test specimens with a double notch in accordance with Miner law and the unified theory.

Based on the unified theory, we represented the curves for various values to obtain the damage development. Each value reflects a loading level. In our case, we have assimilated a fault length (hole diameter plus a notch length) to a loading level. The concavity of the curve is greatest when the loading is low (γ = 1.54) for pierced and simply notched specimens and 2.58 for pierced and doubly notched specimens). But, it tends to follow the linear model of Miner when we increase the level of loading. This parameter takes a very low value for the largest hole diameter, which has been shown in the two figures above. The residual stress, proportional to the non-dimensional number γ, decreases as the hole diameter increases.

The unified theory damage curves are below the Miner law curve. So Miner's law presents more simplicity for the user than the unified theory. For this objective, several researchers have adopted this law for the study of the damage.

5.6 Comparison of the Two Damage Estimation Methods

Figures 18 and 19 represent the correlation between the damage calculated from equation (3) of static damage, that of equation (1) of the unified theory, and the linear damage of Miner. The damages are representative until a life fraction of 40% for pierced and simply notched specimens and 13% for pierced and double-notched specimens. Beyond these values, the damages' evolution becomes unstable, and the materials lose almost all of their characteristics until we notice their total embrittlement. The graphs below show that the static damage appears to become more non-linear with increasing fault depth. Moreover, the noticeable damage from a small defect (a small notch defect) is almost considered a linear one. Indeed, the damage is becoming more and more non-linear while the diameter of the hole increases and the depth gets bigger. Furthermore, the impact of the small defects is linear. This correction appears on the curves in Figure-18 for the case of tests on specimens pierced and simply notched, and in Figure-19 for pierced and double-notched specimens.

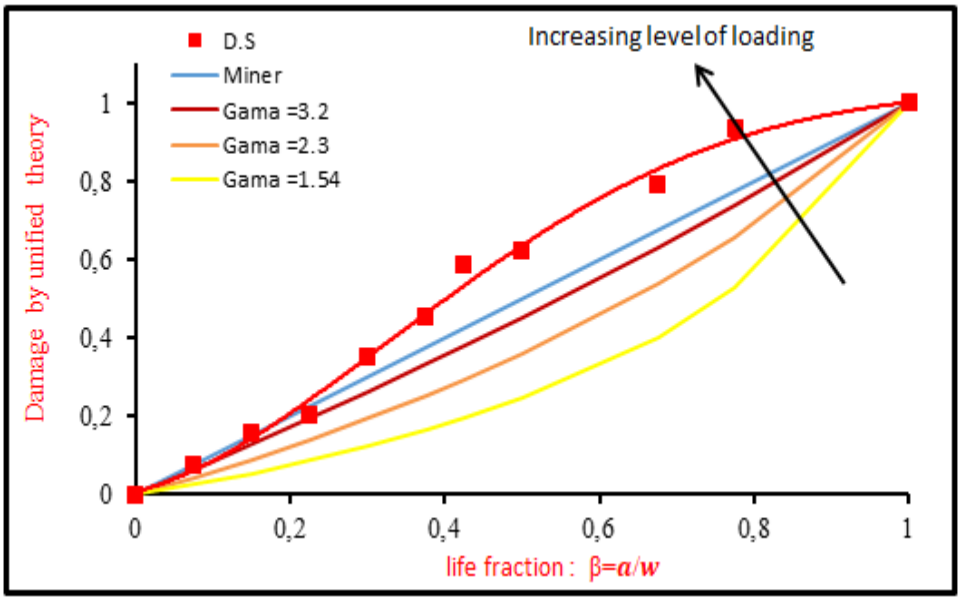

Figure-18. Compares the damage of test specimens punctured with a simple notch with theoretical damage based on the unified theory and the Miner rule depending on the life fraction.

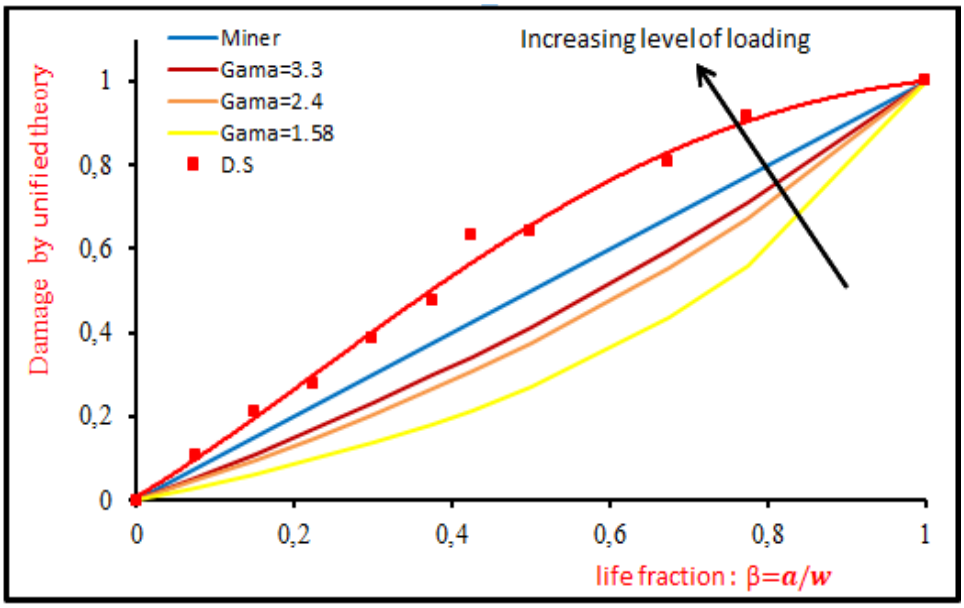

Figure-19. Compares the damage of test specimens pierced with a double notch with the theoretical damage based on the unified theory and the Miner rule depending on the life fraction.

In Figure-18 (specimens pierced and simply notched), it is noted that for the fractions with a short life fraction (0% <β <28%), the experimental damage and the unified theoretical damage at a charge level γ = 1, 5 are similar. The experimental damage curve approaches the MINER damage curve as the life fraction increases, but the experimental damage is considered to be the most critical about all types of damage presented in the two figures, and the correlation between theoretical values and the experimental results of residual stress appears clearly in these two figures. Indeed, we also note the existence of three stages, each of these stages reveals a state and level of ABS damage, and the initial stage is characterized by slow evolution under the theoretical damage up to the life fraction of 20%. We see a continuous rise in the latter in the second stage, reaching 80% of the life fraction. In the last phase, a significant acceleration of the static damage to reach the unit was registered.

6. CONCLUSIONS

On the one hand, the goal of our research is to better understand the characteristics of mechanical behavior of polymers used in industry, particularly ABS, and the parameters that influence this material's behavior to provide solutions to problems encountered during formatting or use. A straightforward tensile test-based analysis of the damage has been offered, and it is simple to implement. Whose aim is to characterize the mechanical properties of virgin ABS specimens and to control the damage of artificially damaged ones? The results show that the presence of defects in the material caused a drop in the residual stress.

The consequences of the identification of the unified damages calculated for various load levels showed that the loading level of 1.9 produced the best results in terms of experimental damage; it appears to be the most realistic to accurately describe the progression of damage to ABS materials with combined defects in hole shape with a single notch and hole shape with a double notch. As well as the three phases of damage development initiation, progression, and acceleration can be determined theoretically using experimental damage, and these stages have been demonstrated to be in good agreement with those discovered empirically.

To reduce intervention costs and increase installation reliability for preventive maintenance, the maintenance department uses the quantification of damage by static damage and unified damage to develop a smart intervention strategy that is implemented at the appropriate time.

NOMENCLATURE

$\gamma_e = \frac{\sigma_e}{\sigma_a}$	:	Non-dimension alendurence limit
$\gamma u = \frac{\sigma u}{\sigma a}$	:	Parameter reflecting the strength of the structure in a virgin state.
$\gamma = \frac{\sigma ur}{\sigma a}$	:	Parameter characterizing the effect of the static damage on the mechanical characteristics of the material.
n	:	Is the instantaneous number of cycles under applied stress.
Nf	:	Is the total number of cycles at the rupture.
σu	:	Limit of the virgin material's endurance
σur	:	is the residual ultimate stress at different hole diameters
σa	:	Applied stress level
and	:	m ; is a material parameter
W	:	is the width of the specimen.
a	:	is the notch depth
D	:	is the damage (D = 0 for neat material, D = 1 for completely damaged material).
β	:	(a/w) = (n/Nf) is the life fraction.

REFERENCES

[1] 2013. Renewable polymeric materials from vegetable oils: a perspective Gerard Lligadas, Juan C. Ronda, Marina Galia` and Virginia Ca´dizMaterials Today. 16(9).

[2] R. Christensen. 1980. Discussion: A Nonlinear Theory of Viscoelasticity for Application to Elastomers. Journal of Applied Mechanics. 47: 682-683.

[3] Bui-Quoc T., Dubuc J., Bazergui A., Biron A. 1971. Cumulative fatigue damage under stress-controlled conditions, J. Basic Eng. Trans.

[4] Henry D. L.1955. A theory of fatigue damage accumulation in steel. Trans. Of the ASME. 1955, 77, 913-918.

[5] Gatts R. R. 1961. Application of cumulative damage concept to fatigue. ASME Journal of Basic Engineering. 83, 529-540.

[6] Lemaitre J., Chaboche J. L. 1979. ANonlinear Model of Creep-Fatigue Damage Cumulation and Interaction. National Office for Aerospace Studies and Research. pp. 1-30.

[7] Zgoul, M. H., Habali, S. M., 2008. An investigation into pipes as hot water transporters in domestic and industrial applications, Jordan Journal of Mechanical and industrial engineering. 2, 191-200.

[8] Joseph V. Rutkowski and Barbara C., USA; Acrylonitrile-Butadiene-Styrene Copolymers (ABS): Pyrolysis and Combustion Products and their Toxicity-A Review of the Literature; Levint us Department of Commerce, National Bureau of

Standards, National Engineering Laboratory, Center for Fire Research, Gaithersburg, MD 20899.

[9] G. M. Domínguez Almaraz, E. Correa Gómez, J. C. Verduzco Juárez J. L., Crack initiation and propagation on the polymeric material ABS (Acrylonitrile Butadiene Styrene), under ultrasonic fatigue testing. Avila Ambriz University of Michoacán (UMSNH), Santiago Tapia No. 403, Col. Centro, 58000, Morelia, Michoacán, Mexico.

[10] T. J. Bohatka, A. Moet. Crack layer analysis of fatigue crack propagation in ABS polymer. Department of Macromolecular Science, The Case School of Engineering, Case Western Reserve University, Cleveland, OH 44106, USA.

[11] Boldizar A., Möller K. 2003. Degradation of ABS during repeated processing and accelerated aging, Polymer Degradation and Stability. 81, 359-366.

[12] R. Rhanim Mechanical behavior Study of damaged structures of polymers. Digital Calculation / Testing Dialogue. Application to photoelasticimetry2016.

[13] G. H. Arid *et al*. 2016. [13] used a standardized degradation formulation on notched test pieces made of rigid PVC. presented on May 28, 2016.

[14] Fatima Majid, Mohamed Elghorba. 2018. Continuum damage modeling through theoretical and experimental pressure limit formulas. Frattura ed Integrità Strutturale, 43, 79-89; DOI: 10.3221/IGF-ESIS.43.05

[15] En-naji A. and al. 2019. Prediction of the thermomechanical behavior of acrylonitrile butadiene styrene using a newly developed nonlinear damage-reliability model. Frattura ed Integrità Strutturale, 49, 748-762; DOI: 10.3221/IGF-ESIS.49.67

[16] En-naji A. and al. 2019. The mechanical characterization and the failure analysis of ABS materials subjected to static tests under the effect of temperature. Key Engineering Materials. ISSN : 1662-9795, Vol. 820, pp 159-172.

[17] En-naji A. and al. 2019. The experimental prediction of the lifetime of Acrylonitrile Butadiene Styrene (ABS) by the Energetic Method. Key Engineering Materials ISSN: Key Engineering Materials. ISSN: 1662-9795, Vol. 820, pp 147-158.

[18] ASTM D638-03 Standard test method for tensile properties of plastics.

[19] ASTM D882 - 02 Standard Test Method for Tensile Properties of Thin Plastic Sheeting.

[20] ASTM D5766 / D5766M Standard Test Method for Open-Hole Tensile Strength of Polymer Matrix Composite Laminates.

[21] M. Miner M. 1945. Cumulative damage in fatigue. Journal of Applied Mechanics. 67: A159-A164.

[22] R. Christensen. 1980. Discussion: A Nonlinear Theory of Viscoelasticity for Application to Elastomers. Journal of Applied Mechanics. 47: 682-683.

[23] K. J. Miller, K. P. Zachriah. 1977. Cumulative damage fatigue crack initiation and state I propagation J. of Strain Analysis. 12(4): 262-270.

[24] Chaboche J. L., Mécanique des matériaux solides 3ème édition, Edition Dunod 2009.

[25] Bui-Quoc T., Du.uc J., Bazergui A., Biron A. 1971. Cumulative fatigue damage under stress-controlled conditions, J. Basic Eng. Trans.

[26] Henry D. L. 1955. A theory of fatigue damage accumulation in steel. Trans. Of the ASME. 1955, 77, 913-918.

[27] Lemaitre J., Chaboche J. L. 1979. ANonlinear Model of Creep-Fatigue Damage Cumulation and Interaction. National Office for Aerospace Studies and Research. pp. 1-30.

[28] Gatts R. R. 1961. Application of cumulative damage concept to fatigue. ASME Journal of Basic Engineering. 1961, 83, 529-540.

[29] J. Dubuc, T. Bui-Quoc, A.Bazergui, A.Biron. 1969. Unified Theory of Cumulative Damage in Metal Fatigue. Rapport soumis à PVRC, vol.Iet II, EcolePolytechnique, avril.

[30] J. Dubuc, T. Bui-Quoc, A. Bazergui, A. Biron. 1971. Weld. Res. Council, PVRC Bulletin 162, juin. pp. 1-20.

[31] Abderazzak Ouardi, Fatima Majid, Nadia Mouhib, Mohamed Elghorba. 2108. Residual life prediction of defected Polypropylene Random copolymer pipes

(PPR), Frattura ed Integrità Strutturale, 43, 97-105; DOI: 10.3221/IGF-ESIS.43.07

[32] En-naji A. and al. 2019. Change Of Experimental Young's Modulus With Increasing Temperature For An Abs Material Subjected To Tensile Test. ARPN Journal of Engineering and Applied Sciences. 14(3), ISSN 1819-6608).

[33] En-naji A. and al. 2018. Change of experimental elongations with increasing temperature for an abs material subjected to tensile test. (IJMET), International Journal of Mechanical Engineering and Technology. ISSN Print: 0976-6340 and ISSN Online: 0976-6359.

[34] SABAH F. and al. 2019. Study of Damage of the Specimens in Acrylonitrile Butadiene Styrene (ABS), Based on a Static Damage Study and Damage by Unified Theory to Predict the Life of the Material. Key Engineering Materials ISSN: 1662-9795, Vol. 820, pp 40-47.

[35] GUGOUCH F. and al. 2019. Damage Prediction of CPVC Based on Energy Method at Different Temperatures. Key Engineering Materials ISSN: 1662-9795, Vol. 820, pp 179-187

[36] Lahlou M. A. and al. 2022. A Numerical Study of the Damage Mechanisms of the Specimens (SENT, SENB, CT, and DENT) used for P265 GH steel. RT&A, No 3 (69)

[37] Khtibari A. and al. 2023. At room temperature, the impact of strain rates on the damage of CVPC compound. Environmental Science and Pollution Research. DOI.org/10.1007/s11356-023-27155-2

[38] Lahlou M. A. and al. 2023. A Numerical Study of the Damage Mechanisms for CT Tensile Specimens of P265GH Steel Material. Periodica Polytechnica Mechanical Engineering DOI.org/10.3311/PPme.20234

[39] Lahlou M. A. and al. 2023. A Study of the Damage Mechanism of Welded CPVC Material. Strength of Materials. DOI: 10.1016/j.prostr.2017.04.041